Accepted Manuscript

Andrew C. Knight, Adrian D. Werner, Dylan J. Irvine
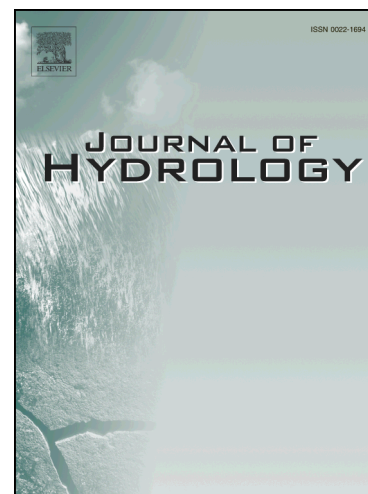
Combined geophysical and analytical methods to estimate offshore freshwater extent

Andrew C. Knight[1,2*], Adrian D. Werner[1,2], Dylan J. Irvine[1,2]

[1]College of Science and Engineering, Flinders University, GPO Box 2100, Adelaide, SA 5001, Australia.

[2]National Centre for Groundwater Research and Training, Flinders University, GPO Box 2100, Adelaide, SA 5001, Australia.

*Corresponding author: Flinders University, GPO Box 2100, Adelaide, SA 5001, Australia.

Tel: +61 8 8201 2657; fax: +61 8 8201 7906.

Email addresses:

Andrew C. Knight: andrew.knight@flinders.edu.au

Adrian D. Werner: adrian.werner@flinders.edu.au

Dylan J. Irvine: dylan.irvine@flinders.edu.au

1

Abstract

Offshore fresh groundwater is increasingly suggested as a potential water resource for onshore human demands. In many cases, onshore pumping already draws significant fresh groundwater from offshore. However, offshore aquifers and the extent of offshore freshwater are usually poorly characterised due to data scarcity. This study combines geophysical data, hydraulic information and a first-order mathematical analysis to investigate offshore freshwater extent in the Gambier Embayment (Australia). A large seismic data set, combined with onshore and offshore bore-log geological profiles, are used to explore the regional offshore hydro-stratigraphy. Aquifer hydraulic parameters and onshore heads are obtained from onshore investigations. A novel application of Archie's law, geophysical data and onshore hydrochemical data provide useful insights into the salinity profiles within four offshore wells. These are compared to steady-state, sharp-interface estimates of the freshwater extent obtained from a recently developed analytical solution, albeit using simplified conceptual models. Salinities derived from resistivity measurements indicate that in the south of the study area, pore water with total dissolved solids (TDS) of 2.2 g L^{-1} is found up to 13.2 km offshore. Offshore pore-water salinities are more saline in the northern areas, most likely due to thinning of the offshore confining unit. The analytical solution produced freshwater-saltwater interface locations that were approximately consistent with the freshwater-saltwater stratification in two of the offshore wells, although analytical uncertainty is high. This investigation provides a leading example of offshore freshwater evaluation applying multiple techniques, demonstrating both the benefit and uncertainty of geophysical interpretation and analytical solutions of freshwater extent.

Keywords: Offshore fresh groundwater; Seawater intrusion; Geophysics; Seismic data; Analytical solution

2

1.0 Introduction

Increasing coastal populations and the impacts of a changing climate are predicted to threaten the freshwater resources of many coastal communities (Post et al., 2013; Michael et al., 2017). Several studies have suggested the use of fresh and brackish water contained within confined and semi-confined submarine aquifers to assist in meeting the freshwater demands of coastal communities (Cohen et al., 2010; Bakken et al., 2012; Post et al., 2013; Jiao et al., 2015). Here, we consider freshwater salinities as total dissolved solids (TDS) < 1 g L^{-1}, while brackish water salinities are 1 g L$^{-1} <$ TDS < 10 g L^{-1}. The landward movement of fresh and/or brackish groundwater stored in subsea aquifers likely delays onshore seawater intrusion (SWI) in several regions globally (Knight et al., 2018). However, as coastal groundwater investigations frequently focus on the onshore resources and coastal fringe processes more generally, the behaviour of fresh groundwater within submarine aquifers remains understudied (Bratton, 2010; Post et al., 2013; Werner et al., 2013).

The occurrence of subsea freshwater and brackish water (referred to collectively as offshore fresh groundwater (OFG) in what follows) is thought to form through two main mechanisms. Firstly, OFG can form where fresh groundwater discharges from an onshore confined or semi-confined aquifer (hereafter termed "semi-confined") into the offshore continuation of the aquifer (Kooi and Groen, 2001; Bakker, 2006). Secondly, increased continental shelf exposure due to vastly different hydraulic conditions during glacial maxima, in some cases leading to increased groundwater hydraulic gradients, are thought to have facilitated the emplacement of freshwater in present-day submarine aquifers (Cohen et al., 2010; Post et al., 2013; Morgan et al., 2018). Both mechanisms require an overlying aquitard to inhibit the

3

rapid vertical mixing of fresh and saline waters that would otherwise occur due to the buoyancy forces induced from seawater overlying freshwater.

Various methods have been applied to assess OFG reserves, although there are few studies that adopt multiple techniques to characterise offshore aquifers for the purposes of freshwater exploration, i.e., to estimate OFG extents. Direct observations of OFG include the sampling of pore-water salinities from offshore core samples (e.g., Jiao et al., 2015), and the sampling of pumped fluids from short-screened intervals offshore (e.g., Krantz et al., 2004). Geophysical methods for characterising OFG include downhole deep-induction resistivity logs and resistivity transect surveys (e.g., Oteri, 1988; Groen et al., 2000; Krantz et al., 2004; Hennig and Otto, 2005). The inverse relationship between resistivity and fluid salinity, contained in Archie's Law (Archie, 1942), can allow for freshwater to be inferred from both transect and downhole resistivity data. However, the method requires knowledge of porous medium resistivities, leading to seldom reported uncertainties in the pore-water resistivities calculated using Archie's law.

There are limited documented studies investigating how regional variations in the hydro-stratigraphy impact offshore salinities. Krantz et al. (2004) used a combination of seismic, resistivity and drill-hole data from aquifers below Indian River Bay (Delaware, USA) to conclude that OFG can preferentially form within sand-filled incised valleys that are silt-capped, with OFG within such channels able to reach several kilometres offshore. Mulligan et al. (2007) identified that when the overlying confining unit is incised by paleo-channels, enhanced vertical flows resulting in increased freshwater-saltwater mixing are likely. Pauw et al. (2017) used onshore data and analytical modelling to demonstrate how shore-parallel variability in the onshore hydro-stratigraphy can alter the OFG extent. Michael et al. (2016)

4

used cross-sectional numerical modelling to show that, in comparison to a homogeneous aquifer, freshwater can extend further offshore in aquifers that have strong vertical heterogeneity but well-connected horizontal flow paths. To date, there is no study supported by offshore data that investigates the potential alongshore variability of OFG extent on a regional scale.

Despite the fact that OFG is considered to be widespread (Post et al., 2013), only three OFG bodies are evidenced by offshore data from the Australian continental shelf, i.e., Perth basin (Hennig and Otto, 2005; Morgan et al., 2018), Adelaide Plains sub-basin (Knight et al., 2018), and Gippsland basin (Varma and Michael, 2012). In all cases, OFG has been found adjacent to significant onshore pumping, which is thought to be mining offshore freshwater to supplement onshore demands (Knight et al., 2018). In the Gambier Embayment (GE), located in the southeast of South Australia (Fig. 1), groundwater supports extensive irrigation schemes and provides water supplies for three coastal towns. Previous studies of the GE suggest that local head conditions in the regional semi-confined aquifer may be conducive to the formation of an extensive OFG body (e.g., Pollock, 2003; Bush, 2009; Morgan et al., 2015), although the occurrence and magnitude of this resource are currently unsubstantiated.
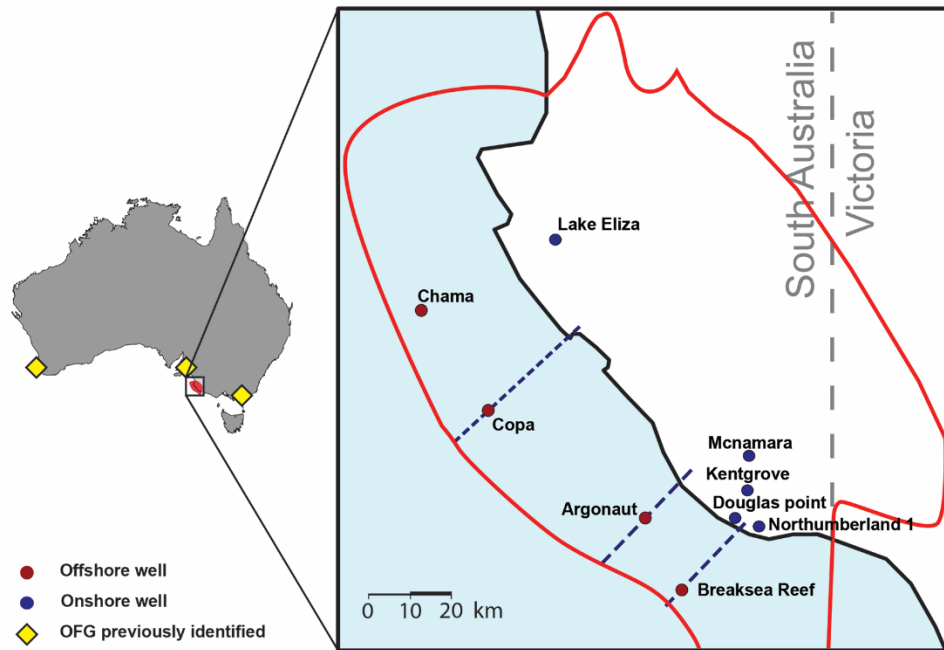
Fig. 1. Regional map showing the location and extent of the GE, delineated by the red line. Current accounts of Australian OFG, identified in existing literature, are marked by yellow diamonds on the national map. Blue and red dots mark onshore and offshore petroleum exploration wells, respectively. Blue dashed lines show the transects used in the current study to apply analytical modelling, herein referred to by the respective wells though which they pass.

Previous studies of the GE by Pollock (2003) and Bush (2009) include offshore interpretations of the main regional semi-confined aquifer (i.e., the Lower Tertiary Confined Aquifer (LTCA)). However, digital copies of the lithological surfaces presented by Pollock (2003) are no longer available and do not separate the LTCA from the overlying confining unit. The hydro-stratigraphic surfaces presented by Bush (2009) terminate at the offshore petroleum exploration well (herein referred to as offshore wells) locations despite the system extending tens of kilometres past the well locations. Neither of these previous seismic studies

6

have generated the hydro-stratigraphic surfaces required to assess the extent of OFG in the GE.

This study aims to provide a best estimate of offshore pore-water salinities in the regional semi-confined aquifer of the GE using available data and through application of the analytical solution of Werner and Robinson (2018). The study also aims to identify the offshore distribution of the upper semi-confined aquifer in the GE, at least at a resolution reasonable for the large scale of the study area, using seismic-line survey data. Knowledge of the offshore hydro-stratigraphy is vital for understanding potential offshore groundwater fluxes, for the interpretation of calculated offshore salinities, and to inform the application of analytical approaches. We aim to establish offshore salinities in the regional semi-confined aquifer of the GE using legacy downhole geophysical data from both onshore and offshore petroleum exploration wells. This study represents the first attempt at using onshore salinity-resistivity relationships to inform the offshore application (and uncertainties) of Archie's law, with the aim of inferring groundwater salinities and the extent of OFG. We compare the salinities calculated from geophysical data against those predicted by analytical modelling to explore the potential influence of present-day hydrological forcing. The Werner and Robinson (2018) analytical solution is applied to a range of conceptual models, each representing simplified versions of the offshore conditions of the GE as determined from available field data.

2.0 Study area

The GE is the western sub-basin of the Otway Basin, an extensive passive rift-sag-rift basin (Boult and Hibburt, 2002) that reaches the city of Melbourne, some 500 km east of the South

7

Australian-Victorian border (Fig. 1). The GE is bounded in the northwest by the Tartwaup Hinge Zone and in the southeast by the Portland Trough (Freeman et al., 2010). The offshore regions of the basin are heavily faulted. Offshore fault lines are generally steeply dipping towards the southwest and have a northwest-southeast strike (Freeman et al., 2010; Holford et al., 2014; Clarke et al., 2015). Previous studies of the GE have identified three hydro-stratigraphic units of importance to anthropogenic activities (Love et al., 1993; Smith et al., 2012; Morgan et al., 2015; Clarke et al., 2015). These are: (1) an Upper Unconfined Aquifer (UUA) comprised primarily of the Gambier Limestone; (2) an Upper Tertiary Aquitard (UTA), consisting of marl intervals and the upper clay layer of the Dilwyn Formation; and (3) a Lower Tertiary Confined Aquifer (LTCA), which encompasses several interbedded, and generally unconsolidated, sand and carbonaceous clay layers of the Dilwyn Formation (Clarke et al., 2015). The UUA, UTA and LTCA are primarily offshore dipping. These units reach a maximum combined thickness of ~1 km in the south of the study area, and thin towards the north (Love et al., 1993). Previous onshore investigations of the GE assume a lower hydro-stratigraphic boundary consisting of the lower clay unit of the Dilwyn Formation in the south, and the Sherbrook Formation (comprising interbedded sands and clays) in the north (Morgan et al., 2015). This lower boundary is based on the assumption that current anthropogenic activities are unlikely to interact with water contained in the Sherbrook Formation (Morgan et al., 2015). We adopt the same assumption in our study.

3.0 Methods

3.1 Offshore stratigraphy from seismic-line surveys

8

In the offshore region of the GE, 32 shore-perpendicular seismic lines and 19 shore-parallel seismic lines were selected for the interpretation of the offshore stratigraphy. Seismic and geophysical well data were obtained from the South Australian Government, Department of the Premier and Cabinet, Energy Resources Division (J. Davies, 2017, pers. comm., 14 December 2017). To generate a regional-scale model of the offshore distributions of the UUA, UTA and LTCA, seismic-line surveys were selected at 3 km spacings in both the shore-parallel and shore-perpendicular directions. Where possible, seismic lines that include multiple well ties (i.e., passing through one or more wells from which downhole lithology has been recorded) were chosen. Seismic data are of varying quality and were acquired at different times. Consequently, it was not possible to determine a minimum resolvable vertical resolution that could be applied to the entire data set. However, previous work using the same data found that seismic reflectors are clearly imaged for units with a two-way travel-time (TWT) under 2000 ms (Freeman et al., 2010). The seismic-line survey data contain no information within 5 km of the shoreline due to a regulatory exclusion zone.

We adopt the methodology used by Pollock (2003) for the interpretation of the hydro-stratigraphic horizons. The top of the UUA, UTA, LTCA, and the Sherbrook Formation were selected to characterise the regional hydro-stratigraphy. As seismic-line surveys have a vertical axis measured in the time domain, a conversion between the measured TWT and depth is required to identify the target horizons on downhole lithology logs. A regional depth-to-TWT relationship of $z = -1132 \times TWT^{1.2678}$ (R^2 of 0.99) was obtained from regression of the available synthetic-seismogram data (i.e., measured TWT values at set depths) from the Breaksea Reef, Chama, and Copa wells (see Fig. 1 for well locations). We use the elevation datum "m AHD" (metres Australian Height Datum), where 0 m AHD is approximately mean sea level. The interpreted seismic horizons for the LTCA were compared against the available

9

hard-copy data presented by Pollock (2003) to ensure that the interpreted seismic sections were equivalent.

Natural-neighbour interpolation was used to generate continuous surfaces for each hydro-stratigraphic unit. Natural-neighbour interpolation was selected due to the linear and clustered characteristics of the seismic-line survey data. The input data consisted of both offshore data points obtained from the tracing of the seismic-line surveys and onshore data points acquired from Morgan et al. (2015). A cell size of 500 m was selected due to the large scale of the study area. The surfaces representing the top of the UTA and LTCA were clipped to honour the extents of these units interpreted from the seismic-line surveys. As this study focuses on the LTCA, the extents of the UUA and pseudo-basement surfaces were restricted to an arbitrarily chosen 10 km from the spatial limits of the available data, as beyond this distance, the surfaces are unlikely to be realistic.

3.2 Calculating offshore groundwater salinities from geophysical borehole logs

3.2.1 Obtaining regional parameters for application of Archie's law

Archie's law (Archie, 1942) is an empirically derived relationship that allows for the calculation of fluid resistivity (r_f) (Ω-m) from a measured bulk resistivity (r_o) (Ω-m) in formations with a relatively non-conductive matrix (e.g., sand, free from clay minerals). Archie (1942) proposed that r_f, r_o, porosity (i.e., total porosity; φ), and a cementation exponent (m) can be related using:

$$r_o = r_f \varphi^{-m} \tag{1}$$

10

In Archie's law, m is related to the degree of connectedness of the pore network (Glover, 2009). A value of $m = 1$ represents a bundle of capillary tubes with all pore spaces connected, while higher values (e.g., 2.5 to 5) represent carbonates with poorly connected pore spaces (Glover, 2009). Typical values of m for sandstone range from 1.3 to 2.6 (Archie, 1942). Values of m are usually established by taking the best-fit slope through a plot of $\log(r_o/r_f)$ versus $\log(\varphi)$ or through re-arranging Eq. 1 to solve for m directly (Glover, 2016).

Despite extensive petroleum exploration within the GE, no pre-existing values of m have been reported within the available literature. Values of m were obtained by applying Eq. 1 to five onshore petroleum exploration wells (Fig. 1) where r_o and lithological data were available. However, values of r_f in the LTCA were unavailable in all the petroleum exploration wells (both onshore and offshore). In addition, no onshore monitoring wells had both φ and r_o data recorded in the LTCA. To apply Eq. 1 to the onshore petroleum exploration wells, values of r_f corrected to 25°C were adopted from the nearest short-screened onshore monitoring well in the LTCA with hydrochemical data available (DEW, 2019). Groundwater salinity measurements elsewhere within the onshore region of the LTCA have low variability over distances similar to the distances between the groundwater monitoring wells where r_f values were obtained and the onshore petroleum exploration wells. For example, the recorded TDS changed by 25 mg L^{-1} between two onshore monitoring wells (well 7022-7871 and well 7021-3339) that were ~10 km apart. The distances between the petroleum exploration wells and the onshore monitoring wells were under 10 km. As r_f data were only available for the upper sand interval of the LTCA, r_o data were also restricted to this interval. The upper sand intervals of the onshore petroleum wells were at similar depths to the screened interval depths in the onshore monitoring wells from which r_f data were obtained. Upper clean sand horizons in each well were identified from downhole lithological

11

descriptions, with gamma ray logs used to discern clean sands from those with significant clay. Using this approach, the GE was found to have clean sand horizons with a gamma ray signature of < 25 API. Lithological descriptions for LTCA sand horizons and the data available for each of the wells used in this study are presented in the Supplementary Material (Table S1). As a variable number of geophysical data points were available within the upper sand horizon in each well, the mean m value for each onshore petroleum exploration well (m_w) was obtained. The regional value for the LTCA of m (m_r) was obtained by taking the mean of the m_w values. The standard deviation of m_r (σ_m) was also obtained.

Porosity can be estimated from both bulk density and sonic logs. Of the wells included in this study, only Argonaut and Chama have both bulk density and sonic logs in the targeted hydro-stratigraphic units. Except for the Copa well, all wells (both onshore and offshore) have sonic log data. A regional value of porosity was used in the application of Eq. 1 to the Copa data because both sonic and bulk density logs were absent at the depths of interest to this study. In the Argonaut and Chama wells where both sonic and density data were available, porosity was preferentially determined for each data point from bulk density logs, according to:

$$\varphi_b = \frac{\rho_m - \rho_b}{\rho_m - \rho_w} \tag{2}$$

Where φ_b is the bulk-density-derived porosity, ρ_m is the density of the solid matrix (~2650 kg m^{-3}; e.g., Groen et al., 2000), ρ_b is the measured bulk density of the saturated porous media (kg m^{-3}), and ρ_w is the density of water (~1000 kg m^{-3}). Excluding the Argonaut, Chama and Copa wells, porosity was determined for each LTCA data point (representing clean sand) from sonic-log data using the Wyllie time-average equation (Wyllie et al., 1958):

$$\varphi_s = \frac{\Delta t_z - \Delta t_{ma}}{\Delta t_f - \Delta t_{ma}} \tag{3}$$

12

Where φ_s is the sonic-derived porosity, Δt_z is the measured acoustic transit time (i.e., the time taken for the seismic wave to travel a unit distance) (μs m^{-1}), Δt_{ma} is the acoustic transit time of the rock matrix (192.9 μs m^{-1}) taken from well completion reports, and Δt_f is the acoustic transit time of interstitial fluids (a value of 616 μs m^{-1} was adopted from the well completion reports). As sonic porosities in unconsolidated sediments tend to overestimate the total porosity, the sonic porosity was divided by a correction factor (c_p), calculated using (Raymer et al., 1980):

$$c_p = \frac{\varphi_s}{\varphi} \qquad (4)$$

The regional value of c_p for the GE was taken as the mean c_p from the Argonaut and Chama wells, for which φ_s were available and φ could be approximated as φ_b values.

In Copa, neither sonic nor bulk-density logs were available in the LTCA. To enable the application of Eq. 1 to the Copa well data, a single regional LTCA φ value was established by taking the mean of the calculated φ values of all data points in the LTCA sand layers (using data from the other eight wells (both onshore and offshore) included in this study).

As electrical resistivity is dependent on temperature, r_o was converted to equivalent values at a standard temperature of 25°C, using (Jorgensen, 1996):

$$r_{25,z} = \frac{1.8(T_z + 39)}{84} r_{o,z} \qquad (5)$$

Where $r_{25,z}$ is the bulk resistivity (Ω-m) adjusted to 25°C at depth z, $r_{o,z}$ is the bulk resistivity (Ω-m) measured at depth z, and T_z is the temperature (°C) at depth z (m). T_z is calculated from the local geothermal profile obtained from drilling completion reports, of:

$$T_z = 0.2759z + 19 \qquad (6)$$

13

3.2.2 Calculating offshore salinity profiles

The downhole r_f profiles of four offshore wells in the GE were calculated by applying a re-arranged form of Eq. 1 to temperature-corrected resistivity data from each well. Temperature corrections were undertaken using Eq. 5. To identify the possible r_f values due to uncertainty surrounding the estimation of m_r, pore-water resistivities were calculated from Eq. 1 using m values of m_r, $m_r \pm 1\sigma_m$, and $m_r \pm 2\sigma_m$. The calculated fluid resistivities were converted to an approximate TDS (mg L^{-1}) at depth z using an empirically derived relationship of:

$$TDS_z = \frac{10,000 \times 0.55}{r_f} \qquad (7)$$

A mean TDS value for each sand interval ($\overline{TDS}$) was established by averaging the calculated pore-water salinities of all the data points contained within each respective sand interval. This was repeated to obtain $\overline{TDS}$ values for all sand intervals, and using alternative values of m (i.e., m_r, $m_r \pm 1\sigma_m$ and $m_r \pm 2\sigma_m$).

3.3 Sharp-interface analytical modelling of present-day steady-state conditions

To explore the possible OFG extent attributable to present-day OFG inflows in the LTCA, the analytical solution of Werner and Robinson (2018) was applied to three simplified shore-normal transects. The Werner and Robinson (2018) solution assumes that the aquifer is flat lying, isotropic, homogeneous, of constant thickness, and is confined onshore and semi-confined offshore. The solution also assumes that: (1) the system is at steady state with respect to onshore heads, (2) the freshwater-saltwater interface can be represented by a line of pressure equilibrium (i.e., a sharp interface), (3) shore-parallel flow is negligible, and (4)

14

vertical freshwater flow in the aquifer can be neglected, while horizontal flow in the semi-confining unit is ignored.

The modelled transects pass through the Breaksea Reef, Argonaut, and Copa wells (Fig. 1). As the interpreted seismic-line survey data indicated that the LTCA and UTA are not continuous between the onshore environment and Chama, the analytical solution of Werner and Robinson (2018) cannot be applied to investigate the potential salinity at Chama from current onshore conditions. Also, the top of the LTCA has an offshore slope of around 1% on average, whereas the analytical solution assumes that the aquifer is horizontal. To account for this, two different sets of geometric conditions (aquifer depth and thickness) were used in applying the analytical solution to each transect, namely: (1) reflecting the conditions at the shoreline, and (2) reflecting the conditions at the offshore wells.

The Werner and Robinson (2018) solution requires the hydraulic conductivity (K) of the aquifer (K_a, m d^{-1}), the thickness of the aquifer (H), the thickness of the semi-confining unit (D), a specified head (h_b) at a distance onshore (x_b), the vertical K of the semi-confining unit (K_l, m d^{-1}), the length of the offshore semi-confining unit (L_s), the depth to the base of the semi-confined aquifer below sea level (z_0), and the densities of fresh (ρ_f, kg m^{-3}) and saline water (ρ_s, kg m^{-3}). The Werner and Robinson (2018) solution allows for the designation of the pore-water salinity of the semi-confining unit, which in this case was set to freshwater, following the recommendation of Solórzano-Rivas and Werner (2017). The parameter sets applied to the Werner and Robinson (2018) solution are listed in Table 1. Parameters obtained from the offshore wells are denoted by an asterisk. Otherwise, parameters reflect onshore data. The analytical solution was applied to both present-day and pre-development heads (h_b and h_b^p, respectively) in the onshore aquifer. Values for h_b^p are approximate only,

and were estimated by extrapolation based on temporal head slopes from earliest recordings (typically in the 1970s). The tip and the toe (where the freshwater-saltwater interface coincides with the aquifer top and bottom, respectively) were obtained by applying the parameters in Table 1 to the analytical solution. Resistivity-derived salinities of TDS $\approx$ 17.5 g L^{-1} (50% of seawater) were used to compare to the tip and toe positions calculated using the sharp-interface analytical solution in the same manner as previous publications (e.g., Werner, 2017).

16

Table 1. Parameters used in applying the Werner and Robinson (2018) solution.

Well	General properties						Onshore properties			Offshore properties		
	K_a (m d^{-1})	h_b (m)	h_b^p (m)	x_b (km)	K_l (m d^{-1})	L_s (km)	H (m)	z_0 (m)	D (m)	H^* (m)	z_0^* (m)	D^* (m)
Breaksea Reef	[a]3.1	[b]17.1	22	0.5	[a]0.0001	33.9	358	694	42	290	905	106
Argonaut	[a]3.1	18.9	22	11.0	[a]0.0001	32.4	415	780	125	356	710	43
Copa	[a]3.1	16.8	23	1.1	[a]0.0001	40.0	73	403	55	46	500	44

[a] Value adopted from Morgan et al. (2015).

[b] Head value averaged from past two years due to a strong seasonal fluctuation.

4.0 Results

4.1 Offshore hydro-stratigraphy

The horizons traced in the seismic-line surveys show evidence of extensive shore-parallel faulting within the offshore hydro-stratigraphic units. Fault-induced displacement appears to have led to localised thinning of the UTA in several survey lines. The interpreted seismic horizons corresponding to the hydro-stratigraphic units for the UTA and the LTCA indicate that the respective units either pinch out underneath the UUA at the continental slope; or remain covered by the UUA rather than terminating at the seafloor. An example of this is visible in Fig. 2a. The northern offshore extent of the UTA and LTCA was determined by considering that these two units appear to onlap (i.e., pinch out) against a local high in the underlying Sherbrook Formation (Fig. 2b), causing the interpreted units to become discontinuous. An example of this onlap is highlighted in Fig. 2b. Other seismic-line surveys

17

that pass through Chama appear to show similar onlap against the Sherbrook Formation in
other directions outwards from the Chama well (see Fig. 3a). This suggests that the UTA and
LTCA recorded in the downhole-lithological log at Chama are disconnected from their
onshore counterparts. Fig. 2a also provides an interpreted cross section of the aquifers of
interest to this investigation. Two additional interpreted cross sections are provided in the
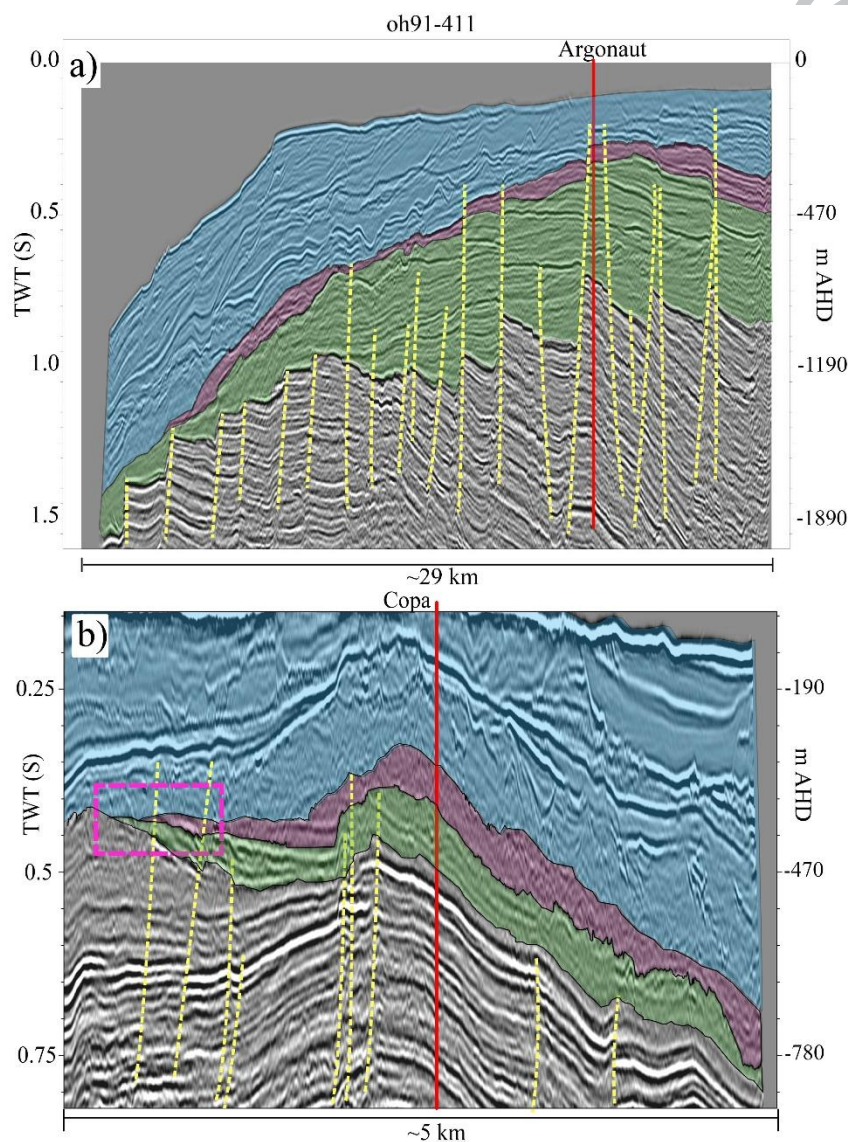Supplementary Material (Fig. S1).

Fig. 2. Seismic-survey lines passing through Argonaut and Copa (upper (a) and lower (b)
panels, respectively). Well locations are marked by the solid red lines, while major

18

interpreted faults are shown by the dashed yellow lines. Blue, pink, and green shading indicate the UUA, UTA, and LTCA units, respectively. Pink dashed box in (b) highlights the area where the UUA and LTCA appear to onlap against the Sherbrook Formation. The locations of seismic-lines are marked in Fig. 3b. The seismic line shown in (a) runs perpendicular to the shoreline from A to A' as marked on Fig. 3. The shoreline is located ~5 km to the right of (a). The seismic line shown in (b) runs parallel to the shoreline from B (northwest) to B' (southeast), also marked on Fig. 3.

The isopach distribution for the UTA and LTCA are shown in Fig. 3. While both the interpolation process and the large cell size chosen acted to dampen high frequency features (e.g., sharp fault-driven elevation changes) in the interpolated offshore hydro-stratigraphic surfaces, there is still noticeable variability regionally in the offshore thickness of the UTA and LTCA. South of Argonaut, the calculated thickness of the UTA (Fig. 3a) varies predominantly between 50 m and 150 m. North of Argonaut, the UTA is mainly 25 m to 100 m thick. The LTCA also displays increased thickness south of Argonaut (Fig. 3b), with thicknesses predominantly between 450 m to 1145 m thick. North of Argonaut, the LTCA thins to between 100 m and 550 m. This northward thinning is also visible in the three interpreted cross sections presented in the Supplementary Materials (Fig. S1). Three paleo-channel features described by Pollock (2003) were interpreted to incise through the UTA and into the LTCA close to the continental slope (Fig. 3a), with the largest of these paleo-channels occurring midway between Copa and Argonaut. As these paleo-channels incise through the UTA, they may reduce the semi-confined offshore extent of the LTCA, and lead to saltwater entering the aquifer preferentially from above. Two maps that display the top of the UTA and LTCA are presented in the Supplementary Material (Fig. S2 and Fig. S3).
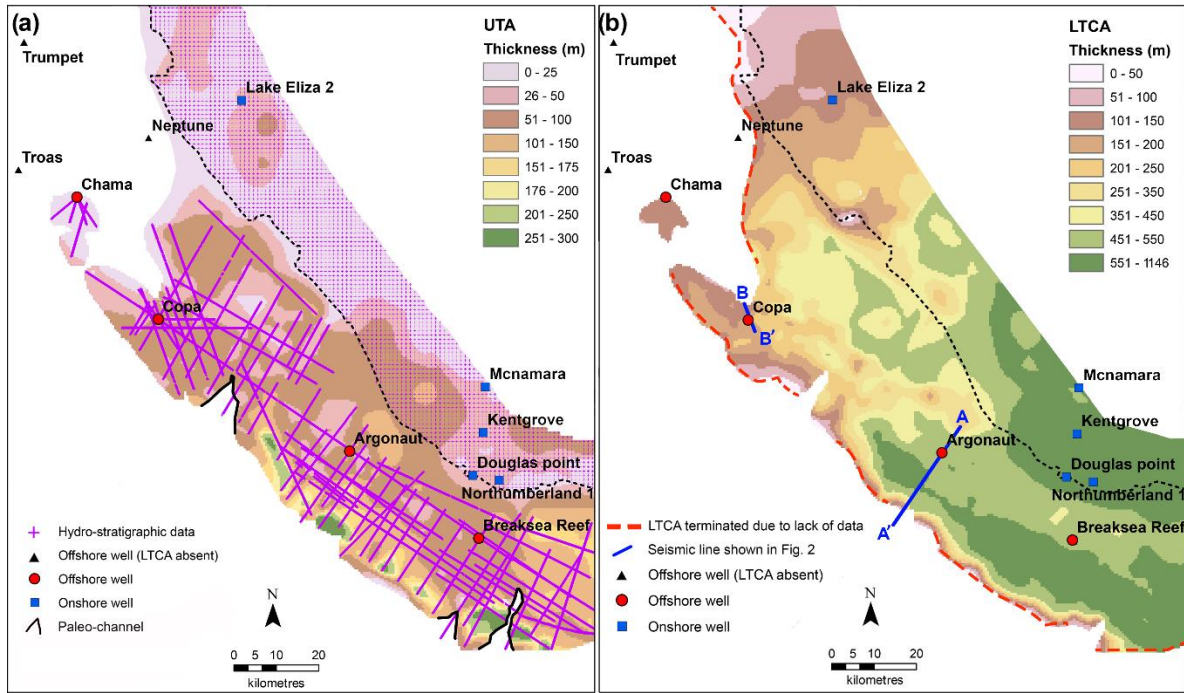
Fig. 3. Isopach maps of (a) the UTA and (b) the LTCA. The blue squares and red dots indicate onshore and offshore wells, respectively. Black triangles indicate offshore wells where the UTA and LTCA are absent in lithological logs. The black-dashed line marks the coastline. In (a), the purple crosses, which appear as purple lines due to their high density, show the data points used in the interpolation of hydro-stratigraphic surfaces. Interpreted paleo-channel extents are marked by solid black lines. In (b), the two seismic-line segments shown in Fig. 2 are marked by blue lines (AA' and BB'), while the red dashed lines indicate where the LTCA and the UTA are terminated due to distance from data points.

4.2 Establishing regional parameters for Archie's Law

Using the onshore petroleum exploration well data, an m_r value of 1.40 and a σ_m of 0.14 were obtained. The regional value of c_p established from paired sonic and density logs was 1.74. The available density and corrected sonic data produced an average φ of 0.37, along with σ_φ (standard deviation of the calculated porosities for LTCA clean sand intervals, extracted from

20

the other eight wells included in this study) of 0.068. There was no clear relationship between

φ and depth, or between m and depth. These data are presented in the Supplementary Material

(Fig. S4 and Fig. S5).

4.3 Offshore salinity profiles from geophysical data

Fig. 4a shows the TDS values for each r_o measurement (limited to sand intervals) in the

Argonaut well. Despite substantial TDS variability, the two shallower sand intervals show

distinctly lower TDS values than the two deeper sand intervals. There is significant scattering

of TDS values within each sand layer. This scattering is greater in the two lower sand

intervals where calculated TDS values are higher. The observed scattering of the calculated

TDS values in an individual sand layer was due to fluctuations in both φ and r_o with depth.

This suggests that a single calculated TDS value is unlikely to be representative of the pore-

water salinities that would be encountered across the entire sand interval.
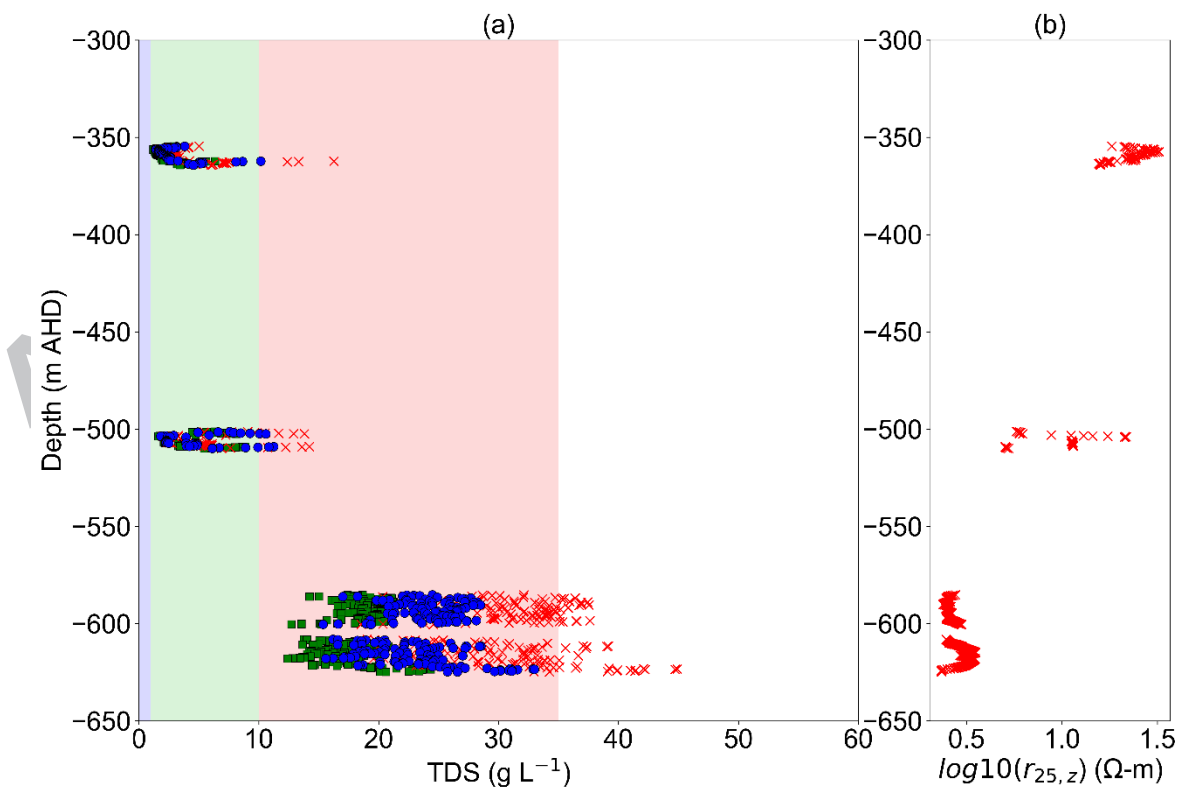
Fig. 4. (a) Calculated TDS values for each r_o measurement of the Argonaut well with depth. Cyan circles, red crosses and green squares show TDS values obtained using m values of m_r, $m_r + 2\sigma_m$ and $m_r - 2\sigma_m$, respectively. Blue, green, and red background shading indicates fresh, brackish, and saline pore water, respectively. White shading indicates a TDS above that of typical seawater. In (b), the temperature corrected r_o values versus depth for Argonaut are displayed. Temperature corrections were undertaken using Eq. 5.

The mean values of TDS ($\overline{TDS}$) for each sand layer in the four offshore wells of interest (Argonaut, Breaksea Reef, Chama and Copa) are presented in Fig. 5. $\overline{TDS}$ calculated using m_r, $m_r \pm \sigma_m$ and $m_r \pm 2\sigma_m$ are shown for each sand interval. The wells ranked in order of the lowest salinity groundwater encountered in each well are: Argonaut, Breaksea Reef, Chama and Copa. The salinities within the Copa well are the highest, with $\overline{TDS}$ in the LTCA ranging between 22.2 g L^{-1} and 30.9 g L^{-1}. The distinctive increase in $\overline{TDS}$ with depth that is apparent at Argonaut (Fig. 4a) can also be found in the Breaksea Reef, Chama and Copa wells, although without the same well-defined salinity stratification of the Argonaut data. For example, the Breaksea Reef data reveal elevated salinities in the uppermost sand interval, for which $\overline{TDS}$ is 11.2 g L^{-1}, while the two underlying sand intervals have a $\overline{TDS}$ of 3.8 g L^{-1} and 4.2 g L^{-1}, respectively. Salinities appear to increase with depth thereafter, with the deepest sand interval in the Breaksea Reef well having a $\overline{TDS}$ of 14.7 g L^{-1}. In Argonaut, salinities increase with depth within the LTCA with a $\overline{TDS}$ of 2.2 g L^{-1} calculated for the shallowest sand interval, while the deepest sand interval in the LTCA has a $\overline{TDS}$ of 22.9 g L^{-1}. In the Chama well, salinity in the LTCA also increases with depth, ranging from 13.1 g L^{-1} in the shallowest sand interval to 45.9 g L^{-1} in the deepest sand interval. There were no sand intervals in Copa that had a $\overline{TDS}$ under 22.2 g L^{-1}.
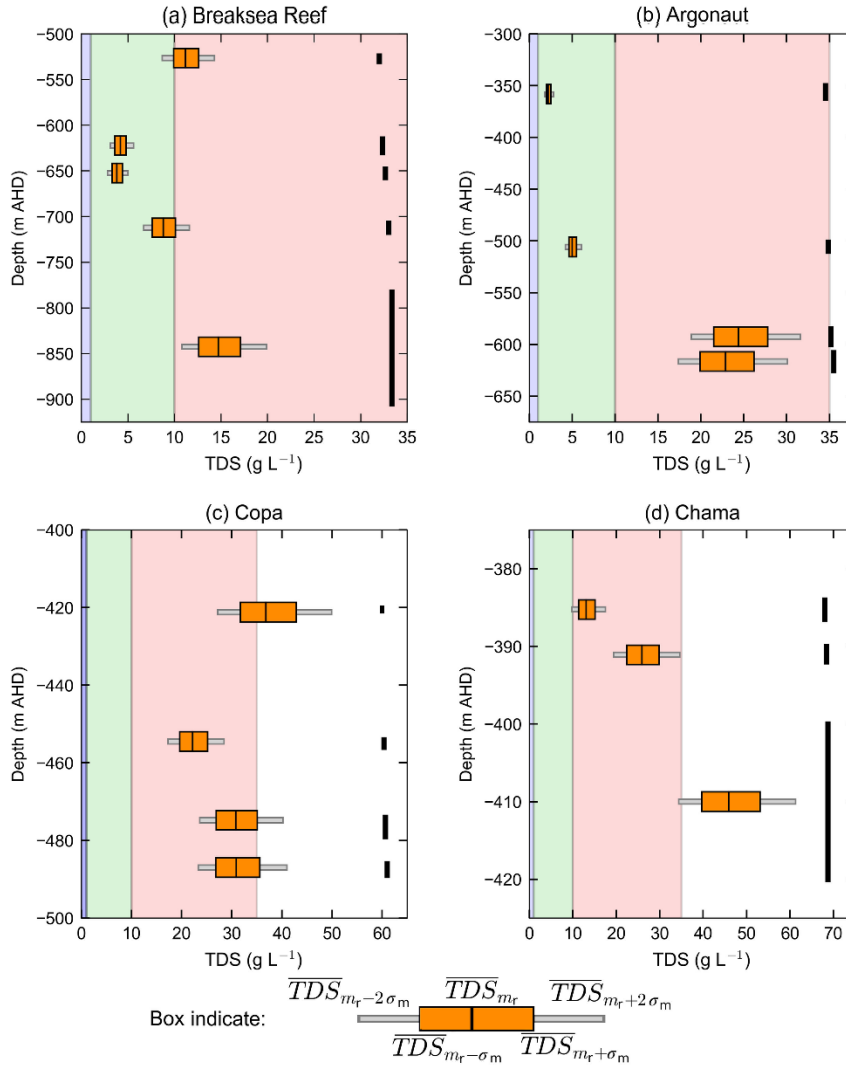
22

Fig. 5. Calculated downhole salinity profiles for the LTCA in the four offshore wells. The red, green, and blue shading indicates, saline, brackish and freshwater, respectively. White background shading indicates that the calculated TDS is above that of typical seawater. The length of the thick black lines on the right-hand side of each plot denotes the thickness of the sand interval captured by the respective box plot. The central line of each orange box shows $\overline{TDS}$ calculated using $m = m_r$, orange box edges show $\overline{TDS}_{m_r \pm \sigma_m}$ which is $\overline{TDS}$ calculated using $m = m_r \pm \sigma_m$, and the outer edges of narrow grey boxes show $\overline{TDS}_{m_r \pm 2\sigma_m}$ which is $\overline{TDS}$ calculated using $m = m_r \pm 2\sigma_m$. Note that scales differ between Fig. 5a-d.

23

4.4 Analytical modelling

The interface tip and toe positions calculated using analytical methods for three transects passing through the Breaksea Reef, Argonaut and Copa wells are listed in Table 2. Four sets of tip and toe positions were produced for each transect using the Werner and Robinson (2018) solution, in accordance with present-day and pre-development conditions, and using cross sections based on onshore and offshore hydro-stratigraphic data.

Table 2. Tip and toe positions calculated using the Werner and Robinson (2018) analytical solution. Positive numbers are offshore while negative numbers are onshore.

Transect	Cross section from onshore data		Cross section from offshore data		Distance to well (km)	Distance to offshore boundary (km)
	Tip (km)	Toe (km)	Tip (km)	Toe (km)		
Pre-development conditions						
Breaksea Reef	33.9	9.0	33.9	-3.4	12.3	33.9
Argonaut	32.4	-1.2	32.4	0.5	13.5	32.4
Copa	29.7	18.9	21.2	14.2	33.6	40.0
Present-day conditions						
Breaksea Reef	33.9	-1.2	10.6	-89.9	12.3	33.9
Argonaut	32.4	-14.7	29.7	-6.6	13.5	32.4
Copa	24.1	13.3	15.8	8.8	33.6	40.0

According to Table 2, calculated toe positions are shoreward of respective well locations for all simulated cases, and therefore, the analytical solution suggests that seawater is at least partly expected to occur in all wells. There is an underlying presumption here that offshore

24

freshwater-seawater conditions are in equilibrium with present-day or pre-development conditions in onshore aquifers. This is discussed further in later subsections. In the Breaksea Reef transect, the application of the analytical solution to present-day conditions produces interface tips that are 33.9 km and 10.6 km offshore for the onshore and offshore data sets, respectively. The calculated present-day steady-state tip positions for the Argonaut and Copa transects follow a similar pattern, with the interface tip calculated using the offshore data, shoreward of those calculated using the onshore data. That is, tip positions from offshore-based aquifer geometries were shoreward of those obtained from onshore geometries by 2.7 km and 8.3 km for Argonaut and Copa, respectively. The tip positions calculated from the present-day onshore data sets for Breaksea Reef and Argonaut both reach the offshore boundary of the semi-confined aquifer. When the Werner and Robinson (2018) analytical solution was applied to the pre-development data sets for Breaksea Reef and Argonaut, the calculated tip reached the offshore boundary for both the onshore and offshore data sets. The analytical solution suggests that under steady-state conditions, present-day onshore heads are capable of driving freshwater past the Argonaut well for both the onshore and offshore parameter sets. For the transect passing through Breaksea Reef, the onshore parameter set indicates that modern heads are sufficient to drive freshwater seaward of the well location, while the offshore parameter set places the tip ~2 km shoreward of the well.

In the Copa transect, the calculated pre-development tip positions are seaward of their present-day counterparts, as expected given the higher pre-development head. However, pre-development tip locations are shoreward of the Copa well location (indicating only seawater in the aquifer at the Copa well location) for both the onshore and offshore data sets. Modern heads were also insufficient to drive freshwater to Copa for either parameter set.

25

5.0 Discussion

5.1 Offshore Salinities of the GE

While potable (TDS < 1 g L^{-1}) water was not identified in the offshore wells included in this study, the low calculated salinities ($\overline{TDS}$ 2.2 g L^{-1}) up to 13.5 km offshore suggest that in the south of the GE, potable water may extend a significant distance offshore. These results support the inferences of earlier work (Pollock, 2003; Bush, 2009; Morgan et al., 2015) that there is a potential for OFG in the GE. The downhole salinity profiles within the LTCA in Breaksea Reef and Argonaut are typical of those observed in other OFG bodies (e.g., Groen et al., 2000; Cohen et al., 2010; Post et al., 2013), in which the salinity generally increases with depth, albeit the transition is not necessarily smooth. The sand intervals in Copa return lower resistivity values than the surrounding clay intervals (data not shown). Under constant pore-water salinities, clays typically return lower resistivity values than sands (Waxman and Smits, 1968), and therefore, the clay pore water is potentially fresher than that in the adjacent sand intervals. This may indicate that clays contained entrapped, fresher pore water, as might occur when more permeable sands salinise due to the landward movement of saline groundwater (e.g., due to falling onshore heads). The observation that clays likely contained fresher water than overlying/underlying sand units may provide useful information on transient interface movements in future investigations of the GE offshore domain.

Using the value of m_r obtained from the LTCA sand layers, preliminary investigations of the possible pore-water salinities in the underlying Sherbrook formation were also undertaken. However, as m_r was established for the LTCA, these values have higher uncertainty. An expanded version of Fig. 5 that includes approximate pore-water salinities of the upper

26

Sherbrook Formation is presented in the Supplementary Material (Fig. S6). Except for a

single sand layer in Chama that has a $\overline{TDS}$ of 11.1 g L^{-1}, the sand layers in the underlying

Sherbrook Formation have approximate calculated $\overline{TDS}$ values in the saline range (i.e., $\overline{TDS}$

between 16.7 g L^{-1} and 46.9 g L^{-1}). No clear relationships between salinity and depth are

apparent in the $\overline{TDS}$ values for the sand layers of the Sherbrook Formation.

The two separate zones of near-brackish water ($\overline{TDS}$ values of 11.1 g L^{-1} and 13.1 g L^{-1}) in

the downhole salinity profile for Chama (Fig. S6d) do not conform to the salinity profile

expected if these two zones are hydraulically connected and/or maintained through

freshwater flow driven by present-day onshore heads. If the two units were hydraulically

connected, then buoyancy forces due to density contrasts between fresh and saltwater, would

cause the brackish water in the lower zone to migrate upwards. Therefore, it appears that

some separation between units of differing hydraulic conductivity is apparent around Chama.

The two southern wells (Breaksea Reef and Argonaut) that contain fresher pore water are

both closer to the shoreline and further from any termination of the UTA than the two

northern wells. For example, the more saline Copa well is 2 km from the interpreted northern

offshore termination of the UTA. If the LTCA is in contact with the UUA along this zone due

to the lack of UTA (aquitard) between the two aquifers (LTCA and UUA) (e.g., Fig. 2b),

increased groundwater mixing may occur. Similar enhanced mixing due to the incision of

submarine paleo-channels through overlying semi-confining units is described by Mulligan et

al. (2007). This presumes that the overlying UUA is saline, which is evident from

consistently low resistivity values in the downhole resistivity logs. The three paleo-channel

features identified in the seismic-line surveys are situated at significant distance (>19 km)

27

from the offshore wells, and are therefore unlikely to have a significant impact on the calculated downhole salinities.

The steady-state OFG extents calculated using the Werner and Robinson (2018) analytical solution indicate that present-day heads may be sufficient to drive freshwater past Argonaut for both the onshore and offshore data sets. The calculated tip positions from the Werner and Robinson (2018) solution suggest that the low resistivity-derived salinities observed in Argonaut may be a result of relatively modern freshwater inputs from the onshore semi-confined aquifer. While the tip position predicted along the Breaksea Reef transect using onshore data indicates that freshwater driven by present-day heads is capable of reaching the continental shelf. The present-day tip position calculated using offshore data is between Breaksea Reef and the coastline, suggesting that present-day onshore heads are unlikely to maintain the offshore freshwater, evidenced by low pore-water salinities observed in the resistivity data, in its current location. As the calculated pre-development tip locations for both the onshore and offshore Argonaut and Breaksea Reef data sets occur seaward of the respective well locations, it is possible that pre-development groundwater flows may have assisted in maintaining/forming the brackish salinities identified from the downhole resistivity data. As groundwater systems are slow to adapt to hydrological changes (Post et al., 2013), it is questionable if the impact of modern changes to the onshore hydrology have reached these offshore well locations. No data set for the Copa transect generated an interface tip that reached the well location. However, this is in agreement with the resistivity-derived salinity data, as the calculated minimum $\overline{TDS}$ for Copa was > 17.5 g L^{-1} (50% of seawater concentration for comparison with the sharp-interface analytical solution).

28

Both the analytical modelling and the resistivity-derived salinities support previous

conceptual models of the offshore GE (e.g., Bush, 2009), in that OFG in the LTCA has both a

paleo/pre-development component and an active flow component, generated due to present

day onshore conditions. Conceptual diagrams of the three transects modelled using the

Werner and Robinson (2018) solution are presented in Fig. 6. In all three transects, there is

potential for submarine fresh groundwater discharge (SFGD) through the overlying confining

unit for several kilometres offshore. However, as no faults were interpreted to extend through

the entire overlying unconfined aquifer (i.e., the UUA) this discharge is unlikely to form

discrete discharge features on the seafloor. The offshore extent of OFG emplaced under paleo

and/or pre-development conditions is likely being reduced due to the landward movement of

the saltwater-freshwater interface caused by changes in the hydraulic conditions, and through

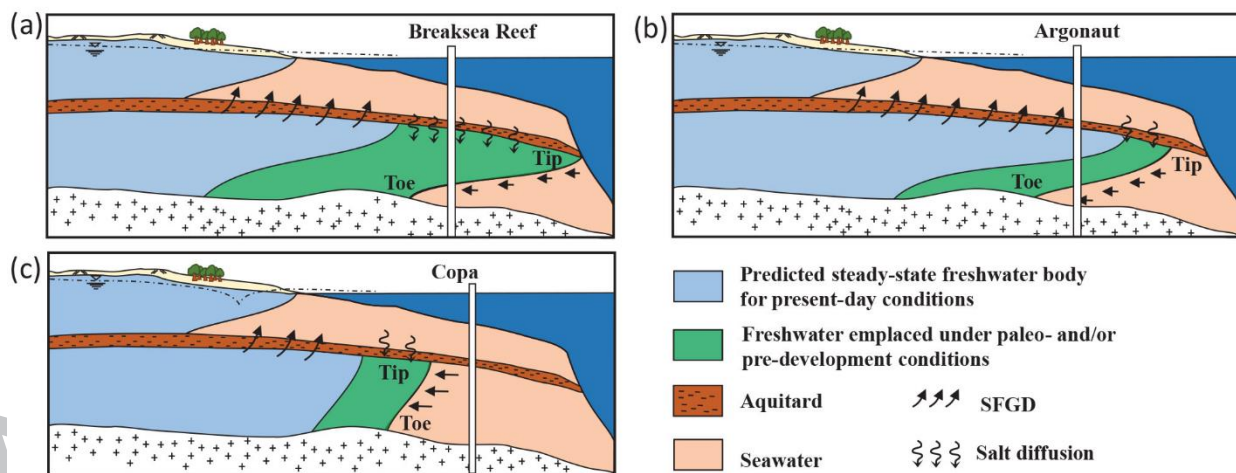the diffusion of salt within the UTA.

Fig. 6. Conceptual representations of the modelled transects, for (a) Breaksea Reef, (b)

Argonaut, and (c) Copa. Note, vertical scales vary. The semi-confined aquifer in (a) is ~300

m thick, (b) ~350 m thick and (c) 50 m thick. Modified from (Knight et al., 2018).

The variability between the tip and toe positions calculated using the onshore and offshore data sets are a result of the variations in z_0, H and D. The depth of the overlying seawater is greater in the offshore data sets in the Breaksea Reef and Copa transects, 211 m and 97 m deeper, respectively. Greater seawater depths result in milder offshore hydraulic gradients (and therefore lower freshwater discharge rates) because increased seawater depths impose greater equivalent freshwater heads on the subsea aquifer. However, in the Argonaut transect, a local offshore topographic high causes a shallower seawater depth (i.e., 70 m shallower) for the offshore dataset, yet the calculated tip and toe positions for the transect using offshore data are landward of the tip and toe positions calculated from the transect using onshore data. This suggests that variations in both H and D must also contribute to the landward shift in the tip and toe positions for the Argonaut transect. All transects generated from offshore data have smaller values of H and D than their onshore derived counterparts. A thinning of the confining unit in the offshore data sets would increase the upwards freshwater leakage through the overlying aquitard in the analytical solution, moving the interface shoreward.

The offshore data sets likely provide a better estimation of the tip position (compared to that obtained using onshore data sets) for the Breaksea Reef and Copa transects, as these data sets capture the thickness of the overlying water column offshore. For the Argonaut transect, the thinner confining unit offshore results in a reduction in the calculated tip position and a reduced estimate of the steady-state freshwater extent. Conversely, when the toe is onshore or close to the shoreline in the GE, it is likely that the onshore data sets provide better estimates of toe positions. This is because the cross sections generated using offshore data may have z_0 values that differ significantly to that identified in the onshore data, resulting in unrealistic calculated toe positions for some offshore transects (e.g., the Breaksea Reef transect that uses offshore data has a toe 89.9 km onshore). The different calculated interface tip positions for

30

the onshore and offshore data sets show that variations in the hydro-stratigraphy make a significant difference to the estimation of subsea interface locations, and that the cross section used to calculate the interface ought to be chosen closest to the expected interface position (e.g., onshore aquifer data for interfaces near the shoreline). In offshore sloping semi-confined aquifers, failure to account for an increase in aquifer depth in the offshore extent has the potential to result in a significant over-estimation of the tip and toe positions if only onshore data are considered in parameterising analytical solutions of the subsea interface.

5.2 Data limitations

Previous studies that have applied Archie's law to obtain pore-water salinities either assume a generic value of m for unconsolidated sediment (e.g., Pauw et al., 2017) or adopt a single value from prior regional studies (e.g., Groen et al., 2000). Locally calibrated m values likely produce more reliable estimates of r_f compared to those obtained from generic values of m. Additionally, consideration of the uncertainty in m that accompanies calibrated values allows for an evaluation of the plausible range in offshore groundwater salinity values. In the LTCA, m_r was 1.40 with a σ_m of 0.14. The difference between the calculated value of m_r (1.40) and the standard value of 1.30 for unconsolidated sands (Archie, 1942) is comparable to σ_m. This indicates that the local variability of m may be high and can have a significant impact on the uncertainty of the final salinity estimates. Additional uncertainty is introduced due to m_r being calibrated from onshore petroleum exploration wells where drilling reports indicate that the drilling muds were freshwater based, yet m_r was applied to calculate salinities in offshore wells where drilling reports indicate that saltwater was used in the drilling mud. While deep induction logs were used to minimise the influence of drilling-induced freshening and/or salinisation of both the invaded zone and borehole fluids, the contrasting borehole drilling-

31

fluid salinities in the onshore and offshore wells may have resulted in the calculated offshore salinities being slightly more saline than the true values. The assumption that the values of r_f in the nearby, onshore monitoring wells are the same as those in the onshore petroleum exploration wells where geophysical data are available generates additional uncertainty. The adoption of r_f values from nearby onshore monitoring wells was necessary as r_f values were unavailable in the onshore petroleum exploration wells that contained the bulk resistivity and porosity data.

The estimates of offshore salinity also incorporate several other possible sources of uncertainty, particularly surrounding the calculation of φ. In the GE, well completion reports note caving of the well walls in sandy zones of the LTCA during drilling. This caving may have caused the calculated porosities to be higher than those observed in the unperturbed LTCA. An overestimation of φ would cause the estimated salinities to be lower than the true values. As both the uncorrected Wyllie time-average equation and the alternative Raymer-Hunt-Gardner equation (Raymer et al., 1980) return unrealistic porosities (i.e., >0.55), the accuracy of the sonic-log derived φ values is questionable. This is despite the more recent Raymer-Hunt-Gardner equation partially correcting for the impact of unconsolidated sediments on sonic velocity data. As both methods originally returned unrealistic porosity estimates, we adopted the Wyllie time-average approach, because this method incorporates a mechanism to scale the sonic-porosity values in unconsolidated sediments, providing that other porosity data such as neutron density-derived porosities are available to estimate correction factors. However, considerable uncertainty is likely to be present due this approach of estimating φ.

32

The tip and toe positions derived from the analytical model are associated with significant uncertainties. These uncertainties arise primarily as a result of numerous simplifications made in the analytical solution that do not fully reflect, the field conditions. As discussed above, the impact of the flat-lying assumption is tested to some degree by the calculation of a tip and toe position for both onshore (where the aquifer is generally shallower) and offshore parameter sets. The cross sections treat H and D as constant across the transect despite the hydro-stratigraphic isopachs (Fig. 3) showing that H and D vary spatially across the GE (e.g., near Argonaut the UTA transitions from a thickness of 25-50 m to a thickness of 100-150 m over a distance of ~5 km). Due to uncertainty surrounding the interpreted hydro-stratigraphic unit thickness, discussed below, H and D in the offshore data sets were obtained from offshore geological well log data. As a result, the spatial variability in H and D was not captured, and the effect of variability on tip and toe positions remains unclear. In addition to regional variations in H and D, the transects used to apply the analytical solution omit multiple shore-parallel faults present in the GE. The localised displacement of the hydro-stratigraphic units associated with this faulting appears to generate several zones where the aquitard thins. These zones of localised thinning generate the potential for increased freshwater/saltwater mixing, which if present may cause the analytical solution to over-predict the OFG extent. However, to date, the impact of a varying aquitard thickness on offshore salinities remains unstudied, and the degree to which these fault-based zones of aquitard thinning impact regional salinities is unknown.

The cross-sectional models treat the LTCA vertically as a single homogeneous unit as per previous regional studies (e.g. Love et al., 1993; Morgan et al., 2015). This is contrary to the downhole geological well data indicating the LTCA is comprised of several sandy layers interbedded with clay, which may have significant thickness in places (i.e., up to 85 m). As

33

the Werner and Robinson (2018) analytical solution is only applicable to the upper-most semi-confined aquifer, it is unclear how this layering would affect the calculated interface position. Michael et al. (2016) found that heterogeneity can result in freshwater driven by onshore heads occurring further offshore than expected in equivalent homogeneous aquifers. However, they did not include a semi-confining unit overlying the homogeneous aquifer, and as a result, their findings apply to a different hydro-stratigraphic arrangement to that adopted by Werner and Robinson (2018).

The offshore stratigraphic interpretations also contain significant uncertainty. The multiple sources of the seismic-line survey data, with variable information surrounding the acquisition parameters, meant that obtaining a minimum vertical resolution was unachievable. As a result, it is likely that the interpreted truncations of the UTA and LTCA do not reflect their true locations, as these units may extend beyond the interpreted end points, albeit at thicknesses below those resolvable from the available seismic data. Confidence in the offshore stratigraphy interpretations is elevated in areas where well ties are possible, particularly around seismic lines that contain multiple well ties. Uncertainty increases rapidly in the offshore direction, as the shore-parallel faulting results in vertical displacement of the seismic horizons, increasing discontinuity in the traced surfaces. Lastly, the seismic exclusion zone imposed between the shoreline and 5 km offshore creates additional uncertainty in the near-shore region. Due to this zone, onshore data were unable to be accurately connected to offshore interpretations.

6.0 Conclusions

34

Our analyses provide a rare demonstration of the significant uncertainty attached to pore-water salinities calculated using Archie's law (Archie, 1942) due to variations of m. We present a new adaptation of methods commonly used in the petroleum industry for establishing m and its variability, to a coastal hydrogeological investigation. In the GE, σ_m was comparable to the difference between m_r and the m value commonly adopted for unconsolidated sands. This highlights the importance of establishing the regional variability of m and not merely adopting the mean m.

We produced estimates of offshore salinity in the South Australian portion of the Gambier Embayment (GE) though novel application of both onshore and offshore geophysical well data. Our analyses indicate that low salinity groundwater ($\overline{TDS}$ ~2.2 g L^{-1}) is likely to be present up to 13.5 km offshore in the south of the GE, albeit there is large uncertainty surrounding this distance. In the north of the GE, calculated pore-water salinities are higher. This suggests that extensive OFG is likely restricted to the southern portion of the GE.

There appears to be a possible association between the offshore hydro-stratigraphy and the calculated salinities, with wells closer to terminations in the UTA and LTCA displaying higher salinities. This may occur due to increased vertical freshwater-saltwater mixing in areas where the LTCA becomes connected to overlying seawater. The seismic-survey data suggests that the LTCA around Copa may be disconnected from the onshore system, highlighting the need to view hydro-stratigraphic and salinity data together to prevent unrealistic extrapolations of OFG bodies in areas where hydro-stratigraphic variability precludes the seaward extent of OFG.

Our analytical modelling indicates that while present-day heads are predicted to drive freshwater significant distances offshore, there is conceptual variability that, when tested within the analytical modelling, leads to significant differences in the estimates of OFG extent. When onshore elevations and thicknesses of the aquifer and aquitard are used for present-day conditions, the calculated steady-state tip position occurs seaward of the Breaksea Reef and Argonaut wells. When elevations and thicknesses that correspond to the offshore well information are used, the calculated interface tip only extends past the well in the Argonaut transect. This indicates that present-day onshore conditions have the potential to explain the occurrence of OFG at Argonaut, while a pre-development OFG component is likely required to explain the calculated salinities at Breaksea Reef. The large discrepancies between calculated tip positions depending on whether onshore or offshore data are used emphasises the need to account for the possible offshore slope of aquifer systems when estimating OFG extents through analytical methods.

Our study presents evidence of a fourth Australian site where OFG is encountered in offshore aquifers. The approach adopted provides a unique example of applying multiple techniques to investigate the potential extent of OFG. Using onshore hydrochemical data, legacy geophysical data and analytical modelling, we were able to approximate offshore salinities, including their uncertainty, and offer hypotheses for OFG origins and influencing factors.

Acknowledgements

36

7.0 References

Archie, G.E., 1942. The electrical resistivity log as an aid in determining some reservoir characteristics. J. Pet. Technol. 5, 1–8. https://doi.org/10.2118/942054-G.

Bakken, T.H., Ruden, F., Mangset, L.E., 2012. Submarine groundwater: a new concept for the supply of drinking water. Water Resour. Manag. 26, 1015-1026. https://doi.org/10.1007/s11269-011-9806-1.

Bakker, M., 2006. Analytic solutions for interface flow in combined confined and semi-confined, coastal aquifers. Adv. Water. Resour. 29, 417-425. https://doi.org/10.1016/j.advwatres.2005.05.009.

Boult, P.J., Hibburt, J.E., 2002. The petroleum geology of South Australia. Vol. 1: Otway Basin. 2nd edn. South Australia Department of Primary Industries and Resources. Petroleum Geology of South Australia Series, 1. ISBN 073-0-841472.

Bratton, J.F., 2010. The three scales of submarine groundwater flow and discharge across passive continental margins. J. Geol. 118, 565-575. https://doi.org/10.1086/655114.

Bush, A.L., 2009. Physical and chemical hydrogeology of the Otway Basin, southeast Australia (Doctoral dissertation). School of Earth Sciences, The University of Melbourne.

Clarke, J.D.A., Lewis, S.J., Fontaine, K., Kilgour, P.L., Stewart, G., 2015. Regional Hydrogeological Characterisation of the Otway Basin, Victoria and South Australia: Technical report for the National Collaboration Framework Regional Hydrogeology

Project. Record 2015/12. Geoscience Australia, Canberra.

https://doi.org/10.11636/Record.2015.012.

Cohen, D., Person, M., Wang, P., Gable, C.W., Hutchinson, D., Marksamer, A., Dugan, B.,

Kooi, H., Groen, K., Lizarralde, D., 2010. Origin and extent of fresh paleowaters on

the Atlantic continental shelf, USA. Ground Water 48, 143-158.

https://doi.org/10.1111/j.1745-6584.2009.00627.x.

Department of Environment and Water (DEW), 2019. Online groundwater data from Water

Connect, as part of DEW, Government of South Australia.

<https://www.waterconnect.sa.gov.au/Systems/GD/Pages/default.aspx> (Cited

27.04.19).

Freeman, B., Boult, P.J., Yielding, G., Menpes, S., 2010. Using empirical geological rules to

reduce structural uncertainty in seismic interpretation of faults. J. Struct. Geo. 32 (11),

1668-1676. https://doi.org/10.1016/j.jsg.2009.11.001.

Glover, P., 2009. What is the cementation exponent? A new interpretation. The Leading Edge

28 (1), 82-85. ISSN 1938-3789. https://doi.org/10.1190/1.3064150.

Glover, P., 2016. Petrophysics MSc. Course Notes. University of Leeds. Accessed on

02/05/2018.

<http://homepages.see.leeds.ac.uk/~earpwjg/PG_EN/CD%20Contents/GGL-

66565%20Petrophysics%20English/Chapter%2016.PDF>.

Groen, J., Velstra, J., Meesters, A., 2000. Salinization processes in paleowaters in coastal

sediments of Suriname: evidence from δ 37 Cl analysis and diffusion modelling. J.

Hydrol. 234, 1-20. https://doi.org/10.1016/S0022-1694(00)00235-3.

Hennig, A., Otto, C., 2005. A hydrodynamic characterisation of the offshore Vlaming Sub-

basin. Research Program, 1.2. Technologies for Assessing Sites for CO2 Storage.

Report No. RPT05-0223. CO2CRC, Canberra. ISBN 978-1-925124-63-7.

38

Holford, S., Tuitt, A., Hillis, R., Green, P., Stoker, M., Duddy, I., Sandiford, M., Tassone, D., 2014. Cenozoic deformation in the Otway Basin, southern Australian margin: implications for the origin and nature of post-breakup compression at rifted margins. Basin Research, 26 (1), 10-37. https://doi.org/10.1111/bre.12035.

Jiao, J.J., Shi, L., Kuang, X., Lee, C.M., Yim, W-S., Yang, S., 2015. Reconstructed chloride concentration profiles below the seabed in Hong Kong (China) and their implications for offshore groundwater resources. Hydrogeol. J. 23, 277-286. https://doi.org/10.1007/s10040-014-1201-6.

Jorgensen, D.G., 1996. The ratio method of estimating water resistivity and TDS from resistivity logs. Groundwater 34 (3), 519-522. https://doi.org/10.1111/j.1745-6584.1996.tb02033.x.

Knight, A.C., Werner, A.D., Morgan, L.K., 2018. The onshore influence of offshore fresh groundwater. J. Hydrol. 561, 724-736. https://doi.org/10.1016/j.jhydrol.2018.03.028.

Kooi, H., Groen, J., 2001. Offshore continuation of coastal groundwater systems; predictions using sharp-interface approximations and variable-density flow modelling. J. Hydrol. 246, 19-35. https://doi.org/10.1016/S0022-1694(01)00354-7.

Krantz, D.E., Manheim, F.T., Bratton, J.F., Phelan, D.J., 2004. Hydrogeologic setting and ground water flow beneath a section of Indian River Bay, Delaware. Ground Water 42 (7), 1035–1051. https://doi.org/10.1111/j.1745-6584.2004.tb02642.x.

Love, A.J., Herczeg, A.L., Armstrong, D., Stadter, F., Mazor, E., 1993. Groundwater flow regime within the Gambier Embayment of the Otway Basin, Australia: evidence from hydraulics and hydrochemistry. J. Hydrol. 143 (3-4), 297-338. https://doi.org/10.1016/0022-1694(93)90197-H.

Michael, H.A., Scott, K.C., Koneshloo, M., Yu, X., Khan, M.R., Li, K., 2016. Geologic influence on groundwater salinity drives large seawater circulation through the

continental shelf. Geophys. Res. Lett. 43 (20).
https://doi.org/10.1002/2016GL070863.

Michael, H.A., Post, V.E.A., Wilson A.M., Werner, A.D., 2017. Science, society, and the
coastal groundwater squeeze. Water Resour. Res. 53, 210-2617.
https://doi.org/10.1002/2017WR020851.

Morgan, L.K., Harrington, N., Werner, A.D., Hutson, J.L., Woods, J., Knowling, M., 2015.
South East Regional Water Balance Project – Phase 2. Development of a Regional
Groundwater Flow Model. Goyder Institute for Water Research Technical Report
15/38. ISSN: 1839-2725.

Morgan L.K., Werner A.D., Patterson A.E., 2018. 'A conceptual study of offshore fresh
groundwater behaviour in the Perth Basin (Australia): Modern salinity trends in a
prehistoric context, J. Hydrol. Reg. Stud. 19, 318-334.
https://doi.org/10.1016/j.ejrh.2018.10.002.

Mulligan, A.E., Evans, R.L., Lizarralde, D., 2007. The role of paleochannels in
groundwater/seawater exchange. J. Hydrol. 335 (3-4), 313-329.
https://doi.org/10.1016/j.jhydrol.2006.11.025.

Oteri, A.U., 1988. Electric log interpretation for the evaluation of salt water intrusion in the
eastern Niger Delta. Hydrolog. Sci. J. 33, 19–30.
https://doi.org/10.1080/02626668809491219.

Pauw, P.S., Groen, J., Groen, M.M.A., van der Made, K.J., Stuyfzand, P.J., Post, V.E.A.,
2017. Groundwater salinity patterns along the coast of the Western Netherlands and
the application of cone penetration tests. J. Hydrol. 551, 756-767.
https://dx.doi.org/10.1016/j.jhydrol.2017.04.021.

Pollock, R.M. 2003. Sequence stratigraphy of the Paleocene to Miocene Gambier Sub-basin,
southern Australia (Doctoral dissertation), University of Adelaide, School of Earth

40

and Environmental Sciences, National Centre for Petroleum Geology and Geophysics and Discipline of Geology and Geophysics.

Post, V.E.A., Groen, J., Kooi, H., Person, M., Ge, S., Edmunds, W.M., 2013. Offshore fresh groundwater reserves as a global phenomenon. Nat. 504, 71-78. https://doi.org/10.1038/nature12858.

Raymer, L.L., Hunt, E.R., Gardner, J.S., 1980. An improved sonic transit time-to-porosity transform: Society of Professional Well Log Analysts 21st Annual Logging Symposium Transactions, paper P, unpaginated. Doc. I.D. SPWLA-1980-P.

Solórzano-Rivas, S.C., Werner A.D., 2017. On the representation of subsea aquitards in models of offshore fresh groundwater. Adv. Water. Resour. 112, 283-294. https://dx.doi.org/10.1016/j.advwatres.2017.11.025.

Smith, P.C., Rogers, P.A., Lindsay, J.M., White, M.R., Kwitko, G. 2012. Gambier Basin, In: Drexel, J.F. and Preiss, W.V. (Eds), The Geology of South Australia. Vol. 2, The Phanerozoic. South Australia. Geological Survey. Bulletin 54, pp. 195-198.

Varma, S., Michael, K., 2012. Impact of multi-purpose aquifer utilisation on a variable-density groundwater flow system in the Gippsland Basin, Australia. Hydrogeol. J. 20 (1), 119-134. https://doi.org/10.1007/s10040-011-0800-8.

Waxman, M.H., Smits, L.J.M., 1968. Electrical conductivities in oil-bearing shaly sands. Soc. Pet. Eng. J. 8 (2), 107−122. https://doi.org/10.2118/1863-A.

Werner, A.D., 2017. Correction factor to account for dispersion in sharp-interface models of terrestrial freshwater lenses and active seawater intrusion. Adv. Water. Resour. 102, 45-52. https://doi.org/10.1016/j.advwatres.2017.02.001.

Werner, A.D., Bakker, M., Post, V.E.A., Vandenbohede, A., Lu, C., Ataie-Ashtiani, B., Simmons, C.T., Barry, D.A., 2013. Seawater intrusion processes, investigation and

41

management: Recent advances and future challenges. Adv. Water. Resour. 51, 3-26. https://doi.org/10.1016/j.advwatres.2012.03.004.

Werner, A.D., Robinson, N.I., 2018. Revisiting analytical solutions for steady interface flow in subsea aquifers: Aquitard salinity effects. Adv. Water. Resour. 116, 117-126. https://doi.org/10.1016/j.advwatres.2018.01.002.

Wyllie M.R.J., Gregory A.R., Gardner L.W., Gardner G.H.F., 1958. An experimental investigation of factors affecting elastic wave velocities in porous media. Geophysics 23 (3), 459–493. https://doi.org/10.1190/1.1438493.

Highlights:

- Novel application of Archie's law used to constrain offshore groundwater salinities.
- Results interpreted in conjunction with seismic data and interface analytical solution.
- New potential Australian offshore fresh groundwater body identified.
- Leading example of offshore freshwater evaluation applying multiple techniques.

49

CRediT author statement

Andrew Knight: Conceptualization, Methodology, Formal Analysis, Investigation, Writing – Original Draft, Visualization. **Adrian Werner:** Conceptualization, Writing – Review & Editing, Supervision. **Dylan Irvine:** Writing – Review & Editing**,** Visualization

Declaration of interests

☒ The authors declare that they have no known competing financial interests or personal relationships that could have appeared to influence the work reported in this paper.

☒The authors declare the following financial interests/personal relationships which may be considered as potential competing interests:

51